

Electric field control of interfacial Dzyaloshinskii-Moriya interaction in Pt/Co/ AlO_x thin films

Marine Schott and Laurent Ranno

*Univ. Grenoble Alpes, CNRS, Grenoble INP,
Institut Nel, 38000 Grenoble, France*

Hélène Béa, Claire Baraduc, and Stéphane Auffret

*Univ. Grenoble Alpes, CEA, CNRS,
SPINTEC, F-38000, Grenoble, France*

Anne Bernand-Mantel*

*Université de Toulouse, Laboratoire de Physique et Chimie des Nano-Objets,
UMR 5215 INSA, CNRS, UPS, 135 Avenue de Rangueil, F-31077 Toulouse Cedex 4, France*

Abstract

We studied electric field modification of magnetic properties in a Pt/Co/ AlO_x trilayer via magneto-optical Kerr microscopy. We observed the spontaneous formation of labyrinthine magnetic domain structure due to thermally activated domain nucleation and propagation under zero applied magnetic field. A variation of the period of the labyrinthine structure under electric field is observed as well as saturation magnetization and magnetic anisotropy variations. Using an analytical formula of the stripe equilibrium width we estimate the variation of the interfacial Dzyaloshinskii-Moriya interaction under electric field as function of the exchange stiffness constant.

*Electronic address: bernandm@insa-toulouse.fr

I. INTRODUCTION

Electric-field (EF) control of magnetism in metals is currently an actively expanding field of study, motivated by potential applications in low power spintronics devices. The magnetization of metallic magnetic materials in spintronics devices can be manipulated using magnetic field or spin-polarized currents flow. The ability to control the magnetic properties of a system using a gate voltage is a promising technique which could lead to the development of EF-assisted magnetization switching devices. Since the first experimental demonstration of EF control of coercive field in a FePt thin film by Weisheit et al. [1], lots of studies have been conducted with the final intention of finding the best conditions for functional devices. Significant variations in the magnetic anisotropy energy under EF application have been observed by many groups [2–7], as well as EF variation of T_c in ultrathin films [8–10]. Recently, the EF impact on the exchange stiffness parameter A_{ex} has been addressed experimentally [11, 12] and theoretically [13]. In these systems, a dielectric oxide layer is present at the top surface of the ferromagnet to allow the application of an EF in a capacitor geometry. This induces a broken spatial inversion symmetry for the ferromagnetic thin film. The presence of these non-identical interfaces is the source of an antisymmetric type of exchange, the Dzyaloshinskii-Moriya interaction (DMI), which has been shown to be a source of chiral spin textures in Pt/Co/ AlO_x for instance [14]. The interfacial origin of this DMI and its consequences in spin textures in ultrathin films make DMI another interesting EF tunable parameter. However, distinguishing EF modulation on DMI from other contributions is not straightforward as direct access to DMI is difficult. In addition to theoretical predictions for ultra-thin samples [15], several experimental studies have reported a change in the DMI factor under EF application [15–20]. This control was shown for relatively thick layers of Fe (20 nm) [16, 20], or a material presenting a weak DMI, Ta/FeCoB/ TaO_x , as demonstrated by Srivastava et al. [17]. More recently, Zhang et al. [19] and Koyama et al. [18] showed larger EF induced variation of DMI in Pt/Fe/MgO and Pt/Co/Pd/MgO systems presenting intermediate DMI values.

In this work, we analyzed labyrinthine domains (also referred to as stripe domains) in samples of Pt/Co/ AlO_x presenting large DMI values [14, 21]. A reversible evolution of the labyrinthine magnetic domain configurations under EF is observed. We also report an EF variation of the saturation magnetization and anisotropy field. The analysis of the variation

of equilibrium stripe width allowed us to estimate the EF variation of the DMI term D . We stress here that this estimation strongly depends on the assumptions made on the exchange constant value.

II. SYSTEM DESCRIPTION AND CHARACTERIZATION

Our system is a Pt(3 nm)/Co(0.6 nm)/AlO_x sputtered trilayer, presenting a gradient of oxidation at the Co/AlO_x interface. This was induced by the post-oxidation of a wedged-shaped Al top layer (Fig. 1(a)). Using this technique, we get access to a low thicknesses range for Co due to the Co partial oxidation in the region where the deposited Al is thin. The sample has been covered by about 50 nm of a high- k insulator, HfO₂, deposited using atomic layer deposition. Then an Indium Tin Oxide (ITO) layer was DC sputtered and patterned in electrodes. These transparent electrodes allow to obtain magneto-optical Kerr effect (MOKE) images of the magnetic domains in the Co layer under a gate voltage (Fig. 1(b)). Voltages of different magnitudes were applied between this top electrode and the Co layer. Here a positive voltage application induces electrons accumulation at the surface of the Co layer (Fig. 1(a)). We used MOKE in polar geometry and recorded images and magnetic hysteresis loops on a single position on the sample through the ITO electrode under different applied voltages (Fig. 1(b)). To determine the EF variation of the saturation magnetization M_s , we measured the variation of the p-MOKE signal between the two opposite saturated states, for out-of-plane applied magnetic field. The average value of magnetization of the wedged sample has been obtained by measuring M_s with a Vibrating Sample Magnetometer-Superconducting Quantum Interference Device (VSM-SQUID). A T_c of 366 K was estimated from VSM-SQUID measurements on the sample under study which possesses an averaged Co thickness of 0.49 nm due to partial oxidation of the deposited Co (see Fig. 1(a)).

A strong EF dependence of M_s is shown in Fig. 1(c). Such sensitivity of the saturation magnetization is due to the proximity of the T_c to the measurement temperature (room temperature). Similar EF control of T_c associated with strong M_s variations were observed in recent studies [11, 22]. The EF variation of the anisotropy field $\mu_0 H_a$ is presented in Fig. 1(d). The anisotropy field $\mu_0 H_a$ is extracted using Stoner-Wohlfarth fit of the magnetization rotation

toward the hard axis direction, on p-MOKE hysteresis loops, for in-plane applied magnetic field. From the measurements of $\mu_0 H_a(V)$, we deduced the variations of the effective magnetic anisotropy energy from the formula $\mu_0 H_a = 2K_{eff}/M_s$, where $K_{eff} = K_s/t - \frac{1}{2}\mu_0 M_s^2$ is the effective magnetic anisotropy and K_s is the surface magneto crystalline anisotropy. A voltage controlled magnetic anisotropy (VCMA) coefficient [23] $\beta_{PMA} = \Delta K_s/\Delta E = 562 \pm 102$ fJ/(V·m) is obtained. This is larger compared to the usual range obtained for a charge accumulation effect (10-290 fJ/(V·m)) [3, 6, 24, 25]. The enhanced effect is again likely due to the proximity of T_c to the measurement temperature.

III. EF VARIATION OF EQUILIBRIUM LABYRINTHINE DOMAINS

As discussed earlier, the analysis of the equilibrium domain configuration has been shown to be one of the ways to study the influence of the EF on different magnetic properties [11, 12]. At zero and negative gate voltages, the domains are blurry due to a very strong thermally induced domain wall motion, as observed in previous works [26]. Thus, in the following we focus our study on positive gate voltages, for which the labyrinthine domains are stable, between 6 V and 14 V. To record the images of labyrinthine states and their variation with the EF, we proceed as follow: under a constant EF, we first saturate the sample with an applied magnetic field, then we turn off the magnetic field and record an image after a waiting time of a few seconds. The images presented in Fig. 2(a)-(d) correspond to the labyrinthine domains which spontaneously appear due to thermally activated nucleation and domain wall propagation. The labyrinthine domains are clearly and reversibly influenced by the application of an EF. The characteristic labyrinthine domain width L_{eq} is estimated using a 2D Fourier transform of the images in Fig. 2(a)-(d). In Fig. 2(e) we present L_{eq} as function of the applied voltage, which shows an increase as a positive voltage is applied to the top ITO electrode. To understand in which way the EF is influencing the domain periodicity, we used an analytical model to describe the domain width L_{eq} in ultrathin films:

$$L_{eq} = C \cdot t \cdot \exp\left(\frac{\pi\sigma_\omega}{2K_d t}\right), \quad (1)$$

where t is the cobalt thickness (which is fixed here to 0.49 nm), K_d the dipolar constant $K_d = \frac{1}{2}\mu_0 M_s^2$ and C is a model-dependent constant [27, 28] of order unity. The experimental domain wall energy σ_ω in Fig. 2(f) is deduced using the measured L_{eq} and M_s values. We

find domain wall energies σ_w around 1.3 – 1.6 mJ/m² for the range of voltages under study, which is consistent with earlier studies [29].

IV. EF VARIATION OF DMI

In the presence of sufficiently strong DMI, the domain wall is of Néel type with a sense of rotation which lowers the domain wall energy [30]: $\sigma_w = \sigma_w^{Bloch} + \sigma_w^{DMI} = 4\sqrt{A_{ex}K_{eff}} - \pi D$, where $D = D_s/t$ stands for the bulk DMI constant and is expressed in J/m², while the surface DMI value D_s is expressed in J/m. We see that in order to extract D using the measured σ_w and K_{eff} values it is necessary to know the exchange constant A_{ex} . We have used two values for A_{ex} . The first value $A_{ex}=7.5$ pJ/m (for $V=0$ V) was deduced from a fit using Kuzmin formula [31] of the temperature dependence of M_s in our sample measured by VSM-SQUID. This reduced value is coherent with recent studies [32]. The second value $A_{ex}=16$ pJ/m (for $V=0$ V) is a value corresponding to bulk thin Co films [33]. The fact that the value of A_{ex} extracted from our VSM-SQUID measurements is lower than the bulk Co value is linked to the low T_c of our sample (366 K) and coherent with the low M_s value. For the same reason we can expect A_{ex} to be influenced by EF as it was already suggested by previous studies [11–13]. We present the different deduced energy terms and their EF variation in Fig. 3. The total domain wall energy σ_w , also shown in Fig. 2(f) is presented in Fig. 3(b). In Fig. 3(a) we present two values and variations of the Bloch wall energy $\sigma_w^{Bloch} = 4\sqrt{A_{ex}K_{eff}}$ deduced from the measured H_a and M_s and the two values of A_{ex} discussed earlier. A_{ex} is considered to vary with EF as $\Delta A_{ex}/A_{ex} = 2\Delta M_s/M_s$, as the general tendency described by mean field approximation is that $A_{ex} \propto M_s^2$ near T_c [34]. Other theoretical studies have found a scaling law of $A_{ex} \propto M_s^{2-\epsilon}$, with ϵ being close to 0.2 for low temperatures [35–37]. Fixing $\Delta A_{ex}/A_{ex} = 2\Delta M_s/M_s$ is then a good approximation and will give us an upper limit for the variation we can expect for $D(V)$. From these assumptions we deduce the DMI value and EF variations which are presented in Fig. 3. The D value at 6 V is ranging between 1.3-2.4 mJ/m² depending on the chosen A_{ex} value. We see that EF variation of σ_w^{Bloch} (Fig. 3(a)) is stronger than the variation of the total wall energy σ_w (Fig. 3(b)) and that an EF variation of D is necessary to compensate this variation (Fig. 3(c)).

To discuss the DMI variations under EF, we use the voltage-control DMI (VCDMI)

seed nm	FM nm	MO _x nm	ΔD mJ/m ²	ΔE MV/m	β_{DMI} fJ/(V·m)	η_{DMI} 10 ⁻¹² J·m/C	ref
Pt 3	Co 0.49	AlO _x /HfO _x 6-53	0.14-0.26 ±0.2	133	1100-2000 ±700	3.9-7.2	here
Ta 3	FeCoB 0.65	TaO _x /AlO _x /HfO _x 1-10-50	0.1	167	600	3.2	[17]*
Ta 3	FeCoB 0.65	TaO _x /AlO _x /HfO _x 1-10-50	0.105	667	158	0.61	[17]
Au 50	Fe 20	MgO/SiO ₂ 10-270	4×10^{-5}	12.5	3.2	1.72	[16]
Pt 4	Fe 2	MgO 367	0.06	800	75	2.65	[19]*
Ta/Pt 2.6-2.4	Co/Pd 0.78-0.4	MgO/HfO _x 2-50	0.038	577	67	0.38	[18]
V/Fe 20-20	Co 0.14	MgO/SiO ₂ 5-50	1.8×10^{-3}	18	100	5.5	[20]
V/Fe 20-20	Co 0.26	MgO/SiO ₂ 5-50	1.2×10^{-3}	18	65	14.5	[38]
Pt	Co 0.6	MgO			26	0.6-1.76	[15]

TABLE I: Summary of DMI variations under EF. The long time scale studies (hours our days) have a star * in the last column.

coefficient [15, 17]), defined as $\beta_{DMI} = \Delta D/\Delta E$ (in J/(V·m), with $\Delta E = \Delta V/t_{Ox}$, where ΔV is the voltage variation and t_{Ox} the dielectric thickness. The coefficient β_{DMI} is plotted versus A_{ex} in Fig. 4. It is in the range of $\beta_{DMI} = 1100 - 2000 \pm 700$ fJ/(V·m). In order to compare this result with previous works we give a summary of the different values in Table 1. Very spread β_{DMI} values between 3.2 and 2000 fJ/(V·m) are obtained. However, these values are not directly comparable, as in addition to different materials and material quality, different thickness ranges of the ferromagnetic layer and different dielectric oxide layers have been used. To obtain comparable values of the (VCDMI) coefficient, we define a new

normalized coefficient η_{DMI} , which we introduce as the variation of surface DMI constant D_s per surface charge provided at the interface of the ferromagnet: $\eta_{DMI} = \Delta D_s / (\epsilon_e \Delta E)$, where ϵ_e is the effective permittivity equal to $\epsilon_e = \epsilon_0 \epsilon_r$ in the case of a single dielectric layer, where ϵ_0 is the permittivity of vacuum and ϵ_r the relative permittivity of the dielectric. This new normalized η_{DMI} coefficient takes into account the fact that the DMI is of interfacial origin, and consequently it is the variation of surface DMI constant D_s which should be compared. In addition, as high-k oxides have been used in order to allow smaller EF for a similar effect on DMI we also have to take into account the effective permittivity of the (possibly multilayered) oxide and compare the effect for a given induced surface charge density and not a given electric field (assuming that the EF effect is induced by electron displacement). After performing this renormalization of the EF changes on DMI, we can now compare the η_{DMI} values corresponding to different studies from several teams. The obtained values lie within the range 0.6 to 14.5×10^{-12} J·m/C. We first see that the two studies with long time scale measurements (made by Brillouin light Spectroscopy (BLS) [17, 19]) provide much larger η_{DMI} . This is potentially due to the ion migration contribution from these long measurements. Long (days or hours) and short time (seconds or minutes) measurements present a factor of 5 ratio in η_{DMI} [17]. Our present result obtained within minute-timescale in ultrathin Co gives intermediate η_{DMI} . For the case of the theoretical paper by Yang et al., we have reported two values for the η_{DMI} , considering or not that the EF calculated corresponds to an applied EF or takes into account the effect of ϵ_r in the oxide, which is still debated in the community, in particular due to the underestimation of the dielectric permittivity of MgO. These two values are thus giving ranges for theoretical η_{DMI} in the Pt/Co/MgO system. The relatively small dispersion in the extracted η_{DMI} values is noticeable, as all these studies have been performed in different teams with samples with different ferromagnetic materials, seed layers and oxides, grown with different techniques (magnetron sputtering or molecular beam epitaxy), measured with different methods (BLS, DW asymmetric motion under in-plane magnetic field, analysis of the labyrinthine domain structures, excitation of magneto-static surface spin-waves) with EF ranging from 18 to 800 MV/m. This indicates that the underlying physics is similar for all these samples despite the very different β_{DMI} proposed. In order to carefully compare interface effect and optimize the EF effect on DMI, one should thus perform calculation of this renormalized, thickness and oxide-independent η_{DMI} .

Conclusion

In conclusion, we were able to deduce a strong EF variation of the magnetic anisotropy energy ($\beta_{PMA} = 562 \pm 102$ fJ/(V·m)) and of the *DMI* term ($\beta_{DMI} \sim 1100 - 2000 \pm 700$ fJ/(V·m)). The strong observed variation of domain size L_{eq} is a result of the combination of variations of every magnetic parameter. The strong β coefficients we were able to deduce for PMA and DMI energies are the result of significantly increased EF effects for measurement temperatures close to T_c .

Acknowledgements

The authors thank M. Chshiev and A. Thiaville for fruitful discussions and C. Mahony for his contribution to the editing of the manuscript. This work was supported by the French ANR via Contract No. ELECSPIN ANR-16-CE24-0018), the DARPA TEE program through Grant MIPR No. HR0011831554 and the EUR Grant NanoX No. ANR-17-EURE-0009 in the framework of the Programme des Investissements d'Avenir.

-
- [1] M. Weisheit, S. Fähler, A. Marty, Y. Souche, C. Poinignon, D. Givord, Electric field-induced modification of magnetism in thin-film ferromagnets, *Science* 315 (2007) 349–351. doi:10.1126/science.1136629.
 - [2] T. Maruyama, Y. Shiota, T. Nozaki, K. Ohta, N. Toda, N. Mizuguchi, A. A. Tulapurkar, T. Shinjo, M. Shiraishi, S. Mizukami, Y. Ando, Y. Suzuki, Large voltage-induced magnetic anisotropy change in a few atomic layers of iron, *Nature Nanotechnology* 4 (2009) 158.
 - [3] W.-G. Wang, M. Li, S. Hageman, C. L. Chien, Electric-field-assisted switching in magnetic tunnel junctions, *Nature Materials* 11 (2012) 64.
 - [4] M. K. Niranjana, C.-G. Duan, S. S. Jaswal, E. Y. Tsybal, Electric field effect on magnetization at the Fe/MgO(001) interface, *Applied Physics Letters* 96 (2010) 222504. doi:10.1063/1.3443658.
 - [5] K. Nakamura, R. Shimabukuro, Y. Fujiwara, T. Akiyama, T. Ito, A. J. Freeman, Giant Modification of the Magnetocrystalline Anisotropy in Transition-Metal Monolayers by an External

- Electric Field, *Physical Review Letters* 102 (2009) 187201. doi:10.1103/PhysRevLett.102.187201.
- [6] M. Endo, S. Kanai, S. Ikeda, F. Matsukura, H. Ohno, Electric-field effects on thickness dependent magnetic anisotropy of sputtered MgO/CoFeB/Ta structures, *Applied Physics Letters* 96 (2010) 212503. doi:10.1063/1.3429592.
- [7] K. Yamada, H. Kakizakai, K. Shimamura, M. Kawaguchi, S. Fukami, N. Ishiwata, D. Chiba, T. Ono, Electric Field Modulation of Magnetic Anisotropy in MgO/Co/Pt Structure, *Applied Physics Express* 6 (2013) 073004.
- [8] H. Ohno, D. Chiba, F. Matsukura, T. Omiya, E. Abe, T. Dietl, Y. Ohno, K. Ohtani, Electric-field control of ferromagnetism, *Nature* 408 (2000) 944–946. doi:10.1038/35050040.
- [9] D. Chiba, S. Fukami, K. Shimamura, N. Ishiwata, K. Kobayashi, T. Ono, Electrical control of the ferromagnetic phase transition in cobalt at room temperature, *Nature Materials* 10 (2011) 853.
- [10] K. Shimamura, D. Chiba, S. Ono, S. Fukami, N. Ishiwata, M. Kawaguchi, K. Kobayashi, T. Ono, Electrical control of Curie temperature in cobalt using an ionic liquid film, *Applied Physics Letters* 100 (2012) 122402. doi:10.1063/1.3695160.
- [11] F. Ando, H. Kakizakai, T. Koyama, K. Yamada, M. Kawaguchi, S. Kim, K. J. Kim, T. Moriyama, D. Chiba, T. Ono, Modulation of the magnetic domain size induced by an electric field, *Applied Physics Letters* 109 (2016) 22401. doi:10.1063/1.4955265.
- [12] T. Dohi, S. Kanai, A. Okada, F. Matsukura, H. Ohno, Effect of electric-field modulation of magnetic parameters on domain structure in mgo/cofeb, *AIP Advances* 6 (2016) 075017. doi:10.1063/1.4959905.
- [13] M. Oba, K. Nakamura, T. Akiyama, T. Ito, M. Weinert, A. J. Freeman, Electric-Field-Induced Modification of the Magnon Energy, Exchange Interaction, and Curie Temperature of Transition-Metal Thin Films, *Physical Review Letters* 114 (2015) 107202. doi:10.1103/PhysRevLett.114.107202.
- [14] M. Belmeguenai, J.-P. Adam, Y. Roussigné, S. Eimer, T. Devolder, J.-V. Kim, S. M. Cherif, A. Stashkevich, A. Thiaville, Interfacial dzyaloshinskii-moriya interaction in perpendicularly magnetized ultrathin films measured by brillouin light spectroscopy, *Physical Review B* 91 (2015) 180405. doi:10.1103/PhysRevB.91.180405.
- [15] H. Yang, O. Boulle, V. Cros, A. Fert, M. Chshiev, Controlling Dzyaloshinskii-Moriya Inter-

- action via Chirality Dependent Atomic-Layer Stacking, Insulator Capping and Electric Field, *Scientific Reports* 8 (2018) 12356. doi:10.1038/s41598-018-30063-y.
- [16] K. Nawaoka, S. Miwa, Y. Shiota, N. Mizuochi, Y. Suzuki, Voltage induction of interfacial Dzyaloshinskii-Moriya interaction in Au/Fe/MgO artificial multilayer, *Applied Physics Express* 8 (2015) 063004. doi:10.7567/apex.8.063004.
- [17] T. Srivastava, M. Schott, R. Juge, V. Kižáková, M. Belmeguenai, Y. Roussigné, A. Bernard-Mantel, L. Ranno, S. Pizzini, S. M. Chérif, A. Stashkevich, S. Auffret, O. Boule, G. Gaudin, M. Chshiev, C. Baraduc, H. Béa, Large-Voltage Tuning of Dzyaloshinskii-Moriya Interactions: A Route toward Dynamic Control of Skyrmion Chirality, *Nano Letters* 18 (2018) 4871–4877. doi:10.1021/acs.nanolett.8b01502.
- [18] T. Koyama, Y. Nakatani, J. Ieda, D. Chiba, Electric field control of magnetic domain wall motion via modulation of the Dzyaloshinskii-Moriya interaction, *Science Advances* 4 (2018). doi:10.1126/sciadv.aav0265.
- [19] W. Zhang, H. Zhong, R. Zang, Y. Zhang, S. Yu, G. Han, G. L. Liu, S. S. Yan, S. Kang, L. M. Mei, Electrical field enhanced interfacial Dzyaloshinskii-Moriya interaction in MgO/Fe/Pt system, *Applied Physics Letters* 113 (2018) 122406. doi:10.1063/1.5050447.
- [20] J. Suwardy, M. Goto, Y. Suzuki, S. Miwa, Voltage-controlled magnetic anisotropy and Dzyaloshinskii-Moriya interactions in CoNi/MgO and CoNi/pd/MgO, *Japanese Journal of Applied Physics* 58 (2019) 060917. doi:10.7567/1347-4065/ab21a6.
- [21] M. Vanatka, J.-C. Rojas-Sánchez, J. Vogel, M. Bonfim, M. Belmeguenai, Y. Roussigné, A. Stashkevich, A. Thiaville, S. Pizzini, Velocity asymmetry of dzyaloshinskii domain walls in the creep and flow regimes, *Journal of Physics: Condensed Matter* 27 (2015) 326002.
- [22] D. Chiba, T. Ono, Control of magnetism in Co by an electric field, *Journal of Physics D: Applied Physics* 46 (2013) 213001.
- [23] B. Dieny, M. Chshiev, Perpendicular magnetic anisotropy at transition metal/oxide interfaces and applications, *Review of Modern Physics* 89 (2017) 25008. doi:10.1103/RevModPhys.89.025008.
- [24] K. Kita, D. W. Abraham, M. J. Gajek, D. C. Worledge, Electric-field-control of magnetic anisotropy of Co_{0.6}Fe_{0.2}B_{0.2}/oxide stacks using reduced voltage, *Journal of Applied Physics* 112 (2012) 33919. doi:10.1063/1.4745901.
- [25] T. Nozaki, A. Koziol-Rachwał, W. Skowroński, V. Zayets, Y. Shiota, S. Tamaru, H. Kubota,

- A. Fukushima, S. Yuasa, Y. Suzuki, Large voltage-induced changes in the perpendicular magnetic anisotropy of an mgo-based tunnel junction with an ultrathin fe layer, *Physical Review Applied* 5 (2016) 044006. doi:10.1103/PhysRevApplied.5.044006.
- [26] N. Bergerard, J. P. Jamet, A. Mougin, J. Ferré, J. Gierak, E. Bourhis, R. Stamps, Dynamic fluctuations and two-dimensional melting at the spin reorientation transition, *Physical Review B* 86 (2012) 1–5. doi:10.1103/PhysRevB.86.094431.
- [27] B. Kaplan, G. A. Gehring, The domain structure in ultrathin magnetic films, *Journal of Magnetism and Magnetic Materials* 128 (1993) 111–116. doi:10.1016/0304-8853(93)90863-W.
- [28] V. Gehanno, Y. Samson, A. Marty, B. Gilles, A. Chamberod, Magnetic susceptibility and magnetic domain configuration as a function of the layer thickness in epitaxial fepd(0 0 1) thin films ordered in the llo structure, *Journal of Magnetism and Magnetic Materials* 172 (1997) 26 – 40. doi:10.1016/S0304-8853(97)00089-9.
- [29] M. Schott, A. Bernand-Mantel, L. Ranno, S. Pizzini, J. Vogel, H. Ba, C. Baraduc, S. Auffret, G. Gaudin, D. Givord, The skyrmion switch: Turning magnetic skyrmion bubbles on and off with an electric field, *Nano Letters* 17 (2017) 3006–3012. doi:10.1021/acs.nanolett.7b00328.
- [30] M. Heide, G. Bihlmayer, S. Blügel, Dzyaloshinskii-moriya interaction accounting for the orientation of magnetic domains in ultrathin films: Fe/w(110), *Physical Review B* 78 (2008) 140403. doi:10.1103/PhysRevB.78.140403.
- [31] M. D. Kuz'min, Shape of Temperature Dependence of Spontaneous Magnetization of Ferromagnets: Quantitative Analysis, *Physical Review Letters* 94 (2005) 107204. doi:10.1103/PhysRevLett.94.107204.
- [32] I. A. Yastremsky, O. M. Volkov, M. Kopte, T. Kosub, S. Stienen, K. Lenz, J. Lindner, J. Fassbender, B. A. Ivanov, D. Makarov, Thermodynamics and Exchange Stiffness of Asymmetrically Sandwiched Ultrathin Ferromagnetic Films with Perpendicular Anisotropy, *Physical Review Applied* 12 (2019) 64038. doi:10.1103/PhysRevApplied.12.064038.
- [33] P. J. Metaxas, J. P. Jamet, A. Mougin, M. Cormier, J. Ferré, V. Baltz, B. Rodmacq, B. Dieny, R. L. Stamps, Creep and flow regimes of magnetic domain-wall motion in ultrathin Pt/Co/Pt films with perpendicular anisotropy, *Physical Review Letters* 99 (2007) 217208. doi:10.1103/PhysRevLett.99.217208.
- [34] U. Atxitia, D. Hinzke, O. Chubykalo-Fesenko, U. Nowak, H. Kachkachi, O. N. Mryasov, R. F.

- Evans, R. W. Chantrell, Multiscale modeling of magnetic materials: Temperature dependence of the exchange stiffness, *Physical Review B* 82 (2010) 134440. doi:10.1103/PhysRevB.82.134440.
- [35] R. Moreno, R. F. L. Evans, S. Khmelevskiy, M. C. Muñoz, R. W. Chantrell, O. Chubykalo-Fesenko, Temperature-dependent exchange stiffness and domain wall width in co, *Physical Review B* 94 (2016) 104433. doi:10.1103/PhysRevB.94.104433.
- [36] Y. O. Kvashnin, W. Sun, I. Di Marco, O. Eriksson, Electronic topological transition and noncollinear magnetism in compressed hcp co, *Physical Review B* 92 (2015) 134422. doi:10.1103/PhysRevB.92.134422.
- [37] I. Turek, J. Kudrnovsk, V. Drchal, P. Bruno, S. Blgel, Ab initio theory of exchange interactions in itinerant magnets, *physica status solidi (b)* 236 (2003) 318–324. doi:10.1002/pssb.200301671.
- [38] J. Suwardy, K. Nawaoka, J. Cho, M. Goto, Y. Suzuki, S. Miwa, Voltage-controlled magnetic anisotropy and voltage-induced dzyaloshinskii-moriya interaction change at the epitaxial fe(001)/mgo(001) interface engineered by co and pd atomic-layer insertion, *Physical Review B* 98 (2018) 144432. doi:10.1103/PhysRevB.98.144432.

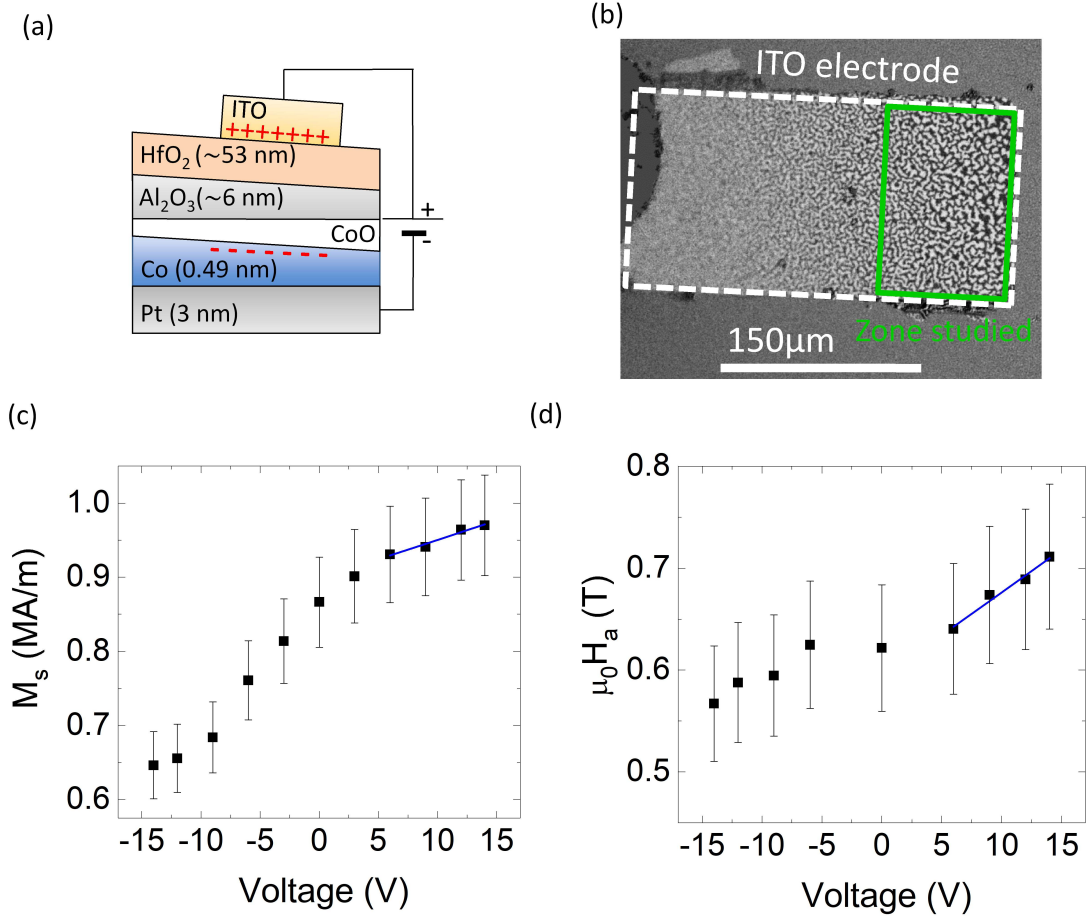


FIG. 1: (a) Schematics of the wedge sample and of the set-up used for EF application: the Pt/Co/AlO_x trilayer is covered by a ~ 50 nm of dielectric layer (HfO₂) and a transparent top electrode (ITO). (b) p-MOKE image of the demagnetized state taken at 0 T, after saturation with an out-of-plane field of 0.4 mT for +12 V applied gate voltage. (c) Evolution of saturation magnetization with gate voltage. A systematic error of 7%, was estimated from the error on the VSM-SQUID measurement. (d) Evolution of anisotropy field with voltage measured from p-MOKE hysteresis loops with in-plane field. A systematic error of 10%, was estimated from fluctuations in the field calibration of the p-MOKE measurement with in-plane applied magnetic field. The blue solid lines in c and d show the regions where the EF-efficiencies have been extracted.

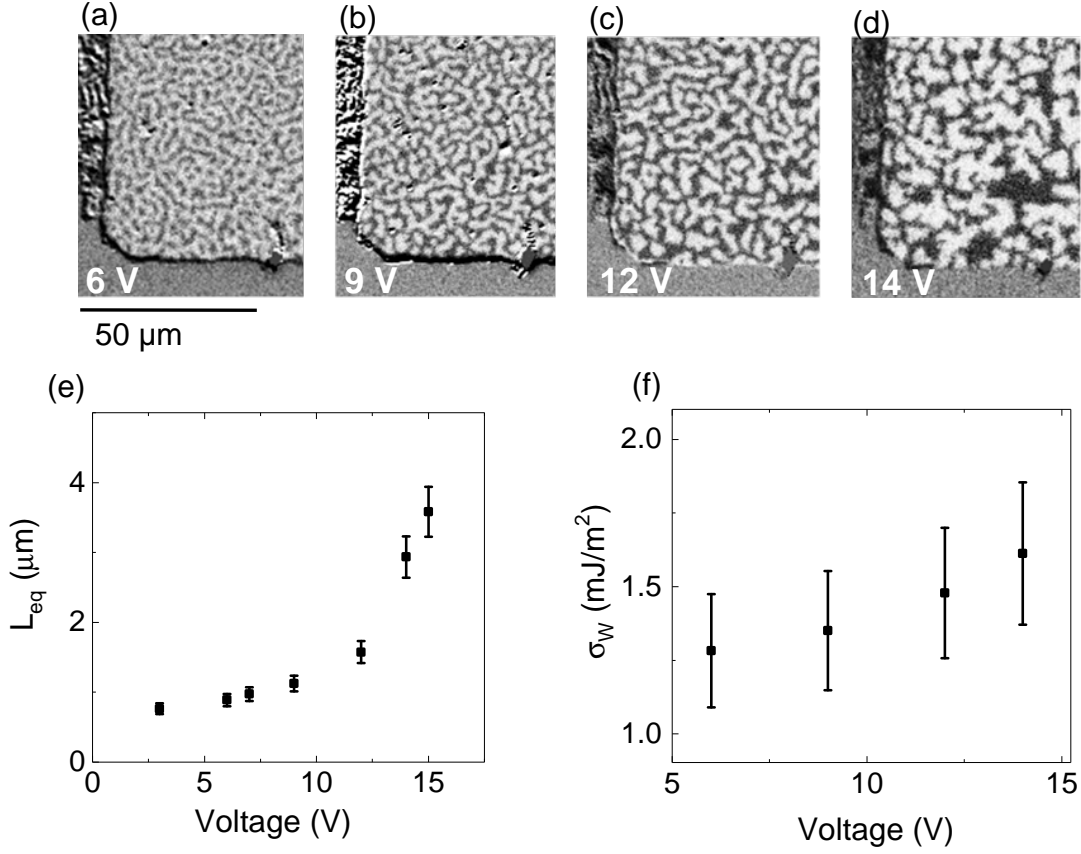


FIG. 2: (a)-(d) p-MOKE images of the evolution of equilibrium stripe width L_{eq} with gate voltage. (e) Equilibrium stripe width L_{eq} as a function of gate voltage. We estimated from repeated measurements a $\sim 10\%$ error on L_{eq} due to imperfect demagnetization. (f) Deduced domain wall energy as function of gate voltage. The error bars correspond to a 16% error calculated from the propagation of the errors in M_s , t and L_{eq} .

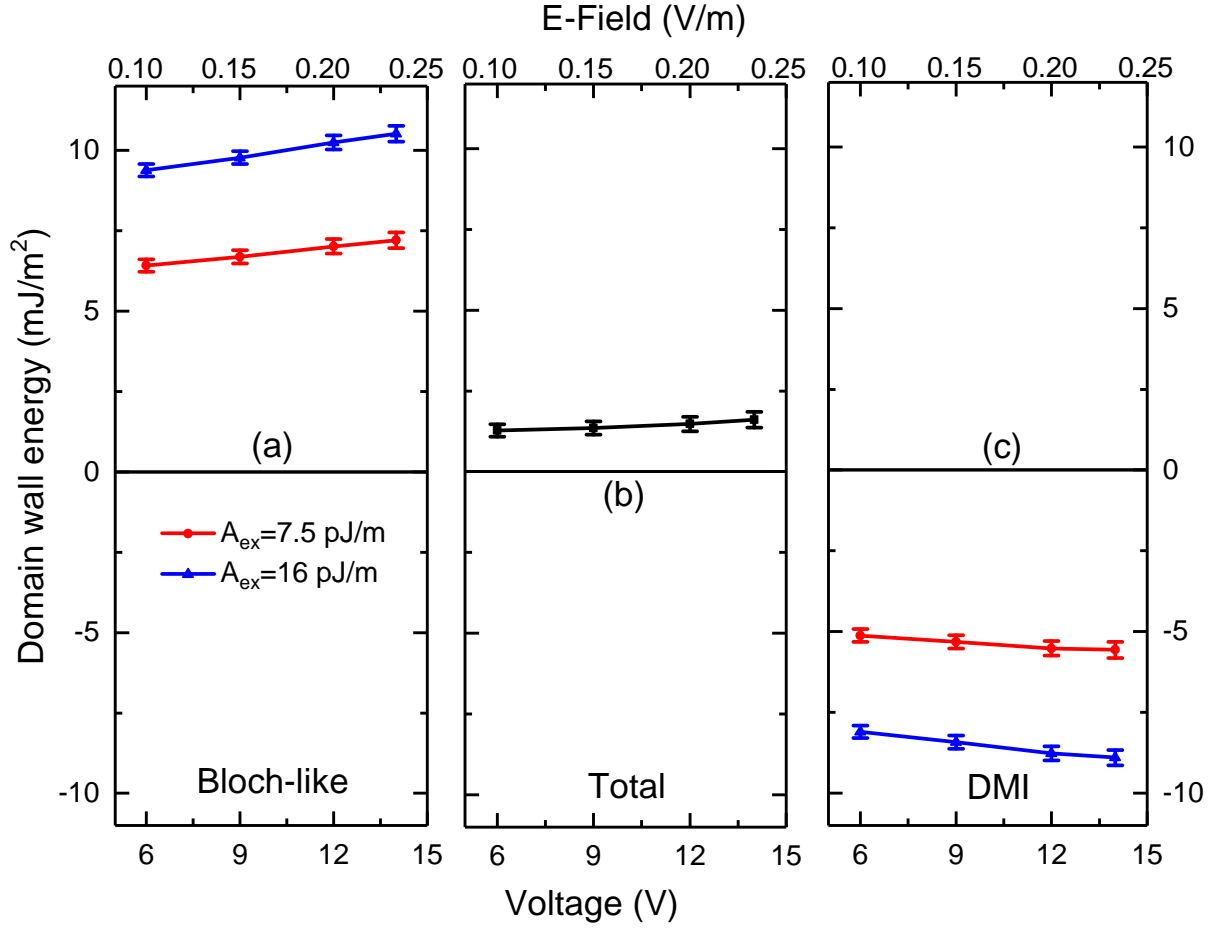


FIG. 3: Different components of the wall energy σ_w as a function of applied EF : (a) Bloch wall energy σ_w^{Bloch} . (b) Total energy σ_w . (c) DMI contribution σ_w^{DMI} .

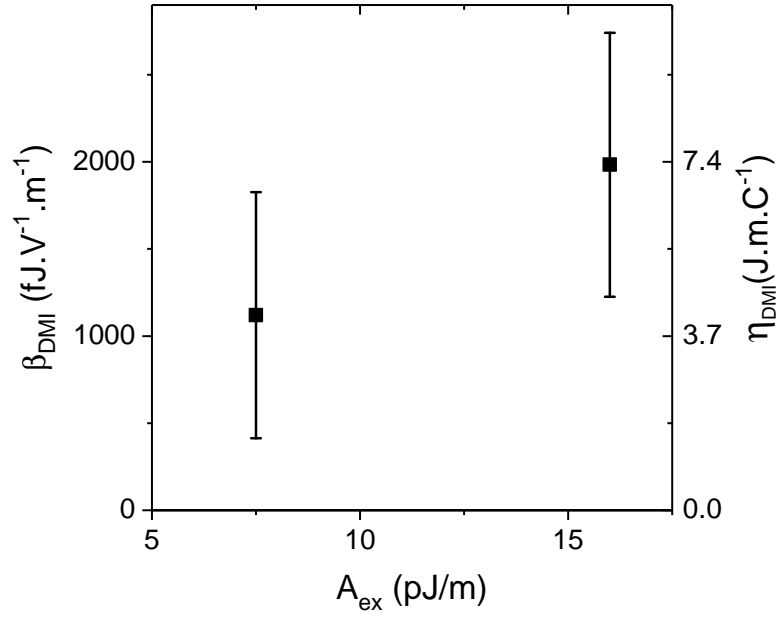


FIG. 4: β_{DMI} coefficients deduced from the experimental M_s , t , L_{eq} and K_{eff} values as a function of the chosen A_{ex} value. The error bars are calculated from the standard error on the slope on a linear fit of $D(V)$.